Comprehensive Toxicity Assessment of PEGylated Magnetic Nanoparticles for *in vivo* applications.

Carlos Caro[a,b,‡], David Egea-Benavente[a,‡], Rocio Polvillo[c], Jose Luis Royo[d], Manuel Pernia Leal[b,*], María Luisa García-Martín[a,*].

[a]BIONAND, Andalusian Centre for Nanomedicine and Biotechnology (Junta de Andalucía-Universidad de Málaga), Málaga, Spain

[b]Departamento de Química Orgánica y Farmacéutica, Universidad de Sevilla, 41012 Seville (Spain)

[c]Andalusian Centre for Developmental Biology, (Universidad Pablo de Olavide-Junta de Andalucia-CSIC). 41013, Seville, Spain,

[d]Area of Biochemistry and Molecular Biology. School of Medicine. University of Malaga. Malaga Spain.

[‡]Carlos Caro and David Egea-Benavente contributed equally to this work.

* email: mpernia@us.es; mlgarcia@bionand.es.

Keywords: magnetic nanoparticles, contrast agents, MRI, toxicity, Zebra fish embryos.

Statistical summary.

Total number of words: 4921

figures: 7

Abstract

Magnetic nanoparticles (MNPs) represent one of the greatest promises for the development of a new generation of diagnostic agents for magnetic resonance imaging, with improved specificity and safety. Indeed, during the last decade the number of studies published in this field has grown exponentially. However, the clinical translation achieved so far has been very limited. This situation is likely related to the fact that most studies are focused on the *in vitro* characterization of these new nanomaterials, and very few provide an exhaustive *in vivo* characterization, where key aspects, such as pharmacokinetics, bioavailability, and, most importantly, toxicity, are properly evaluated. In this work, we propose a protocol for the comprehensive assessment of the toxicity of MNPs, based on the use of Zebrafish embryos as an intermediate screening step between cell culture assays and studies in rodents. MNPs with different cores, ferrite and manganese ferrite oxide, and sizes between 3 and 20 nm, were evaluated. Cell viability at a concentration of 50 μg/mL of PEGylated MNPs was above 90 % in all cases. However, the exposure of Zebrafish embryos to manganese based MNPs at concentrations above 100 μg/mL showed a low survival rate (<50%). In contrast, no mortality (survival rate ~100%) and normal hatching rate were obtained for the iron oxide MNPs. Based on these results, together with the physicochemical and magnetic properties (r_2=153.6 $mM^{-1} \cdot s^{-1}$), the PEGylated 20 nm cubic shape iron oxide MNPs were selected and tested in mice, showing very good MRI contrast and, as expected, absence of toxicity.

1. Introduction

In the last decades, a large part of nanomedicine research has focused on the development of engineered functional nanoparticles (NPs) for *in vivo* applications due to their impressive magnetic, optical or thermal properties, together with improved

biocompatibility.[1-3] These characteristics make NPs excellent candidates for a new generation of diagnostic and/or therapeutic agents, with applicability in many diseases, such as cancer, cardiovascular or neurodegenerative diseases.[4, 5] Among these engineered NPs are the magnetic NPs, which are being thorough studied as a potential new generation of MRI contrast agents for clinical diagnosis.[6-8] However, despite the considerable amount of work devoted to this field of research, a very limited clinical translation has been achieved to date. Indeed, ferumoxytol is currently the only FDA-approved magnetic NPs with potential application as MRI contrast agent in patients with impaired renal function.[9, 10] The reasons underlying this situation are likely related to the fact that many of the studies on MNPs lack crucial information about the *in vivo* behavior of these new nanomaterials, such as their pharmacokinetics, bioavailability, and, most importantly, their toxicity. Although toxicity is one of the key aspects in the characterization of nanomaterials intended for *in vivo* use, most studies on engineered NPs simply report *in vitro* cytotoxicity assays, typically MTT and LDH assays,[11] and very few report *in vivo* toxicity assays.[12] The use of mammalian animal models, typically mice and rats, presents ethical issues due the large number of animals that should be used for the toxicological screening of all the NPs that are being produced. To overcome this limitation, several invertebrate animal models, such as *Caenorhabditis elegans*,[13] *Drosophila melanogaster*,[14] have been used. However, from a translational point of view, vertebrate animal models, specially the Zebrafish (*Danio rerio*), are more appropriate because they exhibit a larger degree of similarity with mammals in terms of early development and signaling repertoire.[15] Thus, the Zebrafish model has emerged as an alternative for *in vivo* toxicological assays of new engineered functional NPs,[16-19] being already well established as a model on environmental sciences.[20, 21] Zebrafish has several advantages over mammalian models, such as the

possibility of performing high-throughput screening due to the high fecundity with rapid embryos development, and the low cost of husbandry and housing. Therefore, the Zebrafish model is an excellent option for *in vivo* toxicity screening of nanomaterials, previous to *in vivo* experiments in mammalian models. Herein, we propose a protocol for the comprehensive toxicity assessment, from *in vitro* to *in vivo*, of MRI contrast agents based on magnetic NPs. MNPs with different cores, ferrite and manganese ferrite oxide, and sizes between 3 and 20 nm, were studied. According to previous studies, the incorporation of the paramagnetic manganese ion in the 3D structure of the NPs induces an enhancement of the magnetic properties of the materials, which could lead to the potential use of the MNPs as T_1 or dual contrast agent, instead of the usual T_2 contrast of the iron oxide MNPs.[22] Following this hypothesis, we prepared both iron oxide and ferrite manganese NPs and compared them in terms of magnetic properties and toxicity. NPs were functionalized with a 3 kDa PEGylated ligand, which enhances their stability in physiological medium without altering their properties. The toxicity of these PEGylated NPs was first assessed *in vitro* on a mouse cell line. Then, Zebrafish embryos were used for *in vivo* toxicity screening. Finally, the most promising magnetic NP was selected and evaluated in mice, including *in vivo* pharmacokinetics and biodistribution experiments by MRI, and histological analysis of tissue sections.

2. Results and Discussion

Synthesis of PEGylated magnetic NPs.

As commented above, in this work we prepared two different sets of magnetic NPs, one of them based on iron oxide and the other one on iron manganese oxide. Each set of NPs was divided on two sizes, small particles around 3 nm and large particles between 14 and 20 nm. The synthesis of the different NPs was carried out following the protocol described

by Hyeon and col.[23] with slight modifications (Figure 1). The subsequent functionalization with a 3 kDa gallol-PEG-OH ligand yielded highly stable monodisperse and water soluble NPs, hereinafter referred to as: Fe1 (3 nm ferrite NP), MnFe1 (3 nm manganese ferrite NP), Fe2 (19 nm ferrite NP) and MnFe2 (14 nm manganese ferrite NP). The presence of the gallol-PEG ligand at the nanoparticle surface was confirmed by FTIR spectroscopy (Figure S1 and S2). The spectra of the functionalized MNPs showed the main peaks of the corresponding gallol-PEG ligand. The hydrodynamic (HD) diameters were measured by Dynamic Light Scattering (DLS) in two media, water and phosphate buffered saline (PBS) to ensure that the stability of the particles remained unaltered at physiological pH and ionic strength (Table S1). The small MNPs, Fe1 and MnFe1, presented HD diameters around 21 nm in water, and slightly larger, between 24-30 nm, in PBS. On the other hand, the large MNPs, Fe2 and MnFe2, presented HD diameters around 56 nm in water, and 63 and 82 nm in PBS, respectively. Therefore, the presence of salt produced small differences in HD diameters, which can be explained by a modification of the hydration/solvation state of the NPs. Moreover, the stability of the MNPs under physiological conditions was studied by measuring the HD diameters in PBS during 24 h, resulting in HD diameters values similar to the initial ones (Figure S3). In addition, the zeta potential of the PEGylated MNPs was slightly negative, which, together with the above results, indicate that these MNPs are highly stable and do not form aggregates in physiological media. To evaluate the potential of these MNPs as MRI contrast agents, T_1 and T_2 relaxivities (r_1 and r_2) were measured at low (1.44 T) and high (9.4 T) magnetic fields, showing similar trends in both cases. The smaller PEGylated Fe1 and MnFe1 exhibited the lower r_2 values, 37.4 and 19.0 $mM^{-1}\cdot s^{-1}$ at 9.4 T and 12 and 6.0 $mM^{-1}\cdot s^{-1}$ at 1.44 T for the Fe1 and MnFe1, respectively. These values are in good agreement with previously reported results for similar magnetic nanoparticles, which

described the correlation between size and magnetic properties, such as r_2 and mass magnetization.[24, 25] On the other hand, as expected, the larger MNPs showed higher r_2 values compared to the smaller ones, 154 and 51 $mM^{-1}\cdot s^{-1}$ at 9.4 T and 80 and 37 $mM^{-1}\cdot s^{-1}$ at 1.44 T for the Fe2 and MnFe2, respectively (Figures S4-S6). The considerable higher r_2 values of the Fe2 are not only due to the larger size, but also to the fact that they exhibit a cubic shape, whereas MnFe2 are spherical. The cubic shape affects the magnetic properties inducing a more ferromagnetic behaviour and therefore higher magnetic susceptibility.[26] Regarding T_1 relaxivity, small and large MNPs behaved differently (Figures S7-S8). At low magnetic field, small MNPs behaved as dual T_1/T_2 contrast agents with r_2/r_1 ratios of 4.8 and 3.8 for Fe1 and MnFe1, respectively. In contrast, large MNPs behaved exclusively as T_2 contrast agents. At high magnetic field, all MNPs showed r_1 values close to 0, restricting their use to T_2 contrast agents (Table S2 and S3).

The cytotoxicity of these engineered MNPs was evaluated *in vitro* using the mouse microglial cell line N13. Cytotoxicity was tested in the concentration range of MNPs between 0.1 to 100 μg/mL (Figure S10). Cultured cells showed no significant cytotoxicity after 24 h of exposure to any of the MNPs, with cell viability values above 90% at a concentration of 50 μg/mL of PEGylated MNPs. These results are in good agreement with previously reported data in which not only iron oxide NPs, but also manganese ferrite NPs did not show any substantial toxicity in different cell lines, such as SMMC-7721[27] or PC-3[24]. Then, before testing the biocompatibility and bioavailability of these potential MRI contrast agents in mice, an *in vivo* toxicity screening was performed on Zebrafish. This approach consisted on the evaluation of the hatching and survival rates of Zebrafish embryos exposed to different concentrations of engineered MNPs (0.01, 0.1, 1, 10, 100 μg/mL) at different times post fertilization (Figure 2a). Regarding the hatching process, control embryos showed around 50% of hatching at 48 h post fertilization (hpf)

(data not shown), in agreement with reported hatching values for normal Zebrafish embryos.[28] Therefore, 48 hpf was selected as the time to assess whether premature hatching occurred in the groups exposed to the MNPs. Higher concentrations of MNPs (10 µg/ml and 100 µg/ml) showed an increased hatching rate in comparison with control non-exposed embryos. As previously reported, this early hatching was probably due to the adsorption of particles on the chorion, which block the pores with the consequent restriction of oxygen and nutrients ~~(Figure 2a)~~.[29] No mortality or malformations were observed in the embryos exposed to different doses of particles at 48 hpf. Another key parameter in the assessment of *in vivo* toxicity is the survival rate of Zebrafish embryos. In the case of iron oxide NPs (Fe1 and Fe2), the survival rate was almost 100% in both cases, in agreement with other studies in which different formulations of water soluble iron oxide NPs were also tested in Zebrafish embryos.[18, 30] However, the survival rate for manganese based NPs (MnFe1 and MnFe2) was 100 % only for low doses, showing a high percentage of mortality for a concentration of 100 µg/mL of MNPs after 6 days post fertilization. (Figure 2b and S11). This toxic effect could be due to a slow release of the Mn cations from the inorganic core, which would lead to neurotoxicity by mitochondrial dysfunction.[31, 32] Similar results have been described for cobalt ferrite NPs, which were proved very lethal even at low concentration.[33] Therefore, mortality of the Zebrafish embryos was found to be nanoparticle type-, dose- and time-dependent. The discordant results obtained between cell cultures and Zebrafish embryos in the case of manganese ferrite NPs demonstrate the importance of including animal models in the toxicity studies of NPs designed for *in vivo* use.

In summary, whereas the *in vitro* cytotoxicity assays in cell culture showed low toxicity for all MNPs, the *in vivo* assays in Zebrafish embryos revealed that only iron oxide nanoparticles are suitable for *in vivo* use. Specifically, only Fe1 and Fe2 were selected as

potential contrast agents for *in vivo* imaging based on their low toxicity. ~~Also, these iron based NPs presented a shape-dependent behaviour in terms of relaxivity.~~ Cubic MNPs showed mainly T_2 contrast at low and high magnetic fields, whereas spherical MNPs showed dual T_1 and T_2 contrast at low magnetic field and only T_2 contrast at 9.4 T. Based on these results, the engineered cubic Fe2 was selected among all NPs as the most promising contrast agent for MRI, being then characterized *in vivo* in Balb/c mice. Thus, Fe2 (5 mg of Fe per kg of body weight) was intravenously injected in the tail vein of Balb/c mice, and followed by MRI.[34] Short term pharmacokinetics (up to 30 min) showed a rapid liver uptake, with a maximum relative enhancement (RE, Figure 3) at one minute after injection. The kidneys also showed a significant RE, which remained almost constant during the 30 min of the dynamic MRI experiment, involving that a significant amount of Fe2 was circulating during this time period, as discussed elsewhere.[24, 35] Moreover, long term pharmacokinetics based on quantitative T_2 mapping showed a clear T_2 decrease in liver and kidneys at 1 h after injection, with ΔT_2 of - 5.5 and -15.8 in liver and kidneys, respectively. These quantitative data further support that, in spite of being partially taken up by the kupffer cells of the liver, a significant amount of Fe2 is still present in the bloodstream after one hour, which means that these MNPs show good bioavailability, as previously described by our group for similar PEGylated magnetic NPs.[36] Finally, the possible side effects produced by the intravenous injection of MNPs were also evaluated by histological analyses. Thus, hematoxylin and eosin stain was performed on tissue samples of liver and kidneys, showing no significant alterations after exposure to Fe2 compared to controls. Liver sections showed normal appearance, without the vacuolated swelling of the cytoplasm of hepatocytes that is typically indicative of acute and subacute liver injury. Similarly, kidneys presented normal tubular brushborders and intact glomeruli surrounding Bowman's capsule, evidential of no kidney injury

(Figure 4).[36, 37] Moreover, the mouse body weight was also followed during 28 days after the administration of Fe2, showing the same pattern as the control group, in agreement with the absence of toxic effect *in vivo* (Figure 4).

3. Conclusion

In conclusion, an exhaustive toxicity screening, based on cell cultures, Zebrafish embryos and mice, is proposed to properly evaluate the toxicity of magnetic nanoparticles developed as potential MRI contrast agents. Our results demonstrate that toxicity tests based on cell cultures alone are not enough to evaluate the toxicity of nanomaterials that are intended for *in vivo* use. Unfortunately, this is a common practice in many of the studies in the field, but in our experience, the use animal models should always be included as part of the protocol to evaluate the toxicity of new nanomaterials for *in vivo* applications. The Zebrafish model is an excellent option as an intermediate screening step to properly evaluate toxicity avoiding the excessive use of rodents. In this work, two different magnetic cores, based on ferrite and manganese ferrite oxides, with different sizes, from 3 to 20 nm, were studied. A detailed characterization on the PEGylated MNPs showed high long term stability, no *in vitro* toxicity and good T_2 and dual T_2/T_1 MRI contrast at high and low magnetic fields, respectively. An intermediate *in vivo* toxicity screening was performed on Zebrafish embryos to select the best candidate for the MRI experiments in mice. No mortality and normal hatching rate were obtained on the Zebrafish embryos exposed to iron oxide NPs. However, in contrast to *in vitro* results, significant toxicity was obtained for magnetic NPs based on manganese ferrite. A low percentage of survival was found on the embryos exposed to the highest concentration of manganese ferrite NPs after 6 days post fertilization. From all the tested MNPs, Fe1 and Fe2 showed the lowest toxicity and between these two, the Fe2 (20 nm cubic shape) presented the best characteristics as a potential MRI contrast agent. Therefore, this MNP

was selected for *in vivo* experiments in mice. Significant MRI contrast enhancement was observed in the liver and kidneys of mice following the intravenous injection of Fe2. The histological analysis of tissue sections and the weight control over several weeks, confirmed the safety of this MNP.

4. Experimental Section

4.1. Materials. Chemicals and solvents were obtained from commercial suppliers (Sigma Aldrich, Acros Organics and Fisher Scientific) and used as received. Iron (III) chloride, Manganese (II) chloride, Sodium Oleate, Oleic acid 99%, Oleic alcohol, ~~Oleylamine~~, ~~Benzyl ether~~, ~~1,2-Hexanedecanediol~~, Gallic acid, Poly ethylene glycol 3000 Da, 1-octadecene, diphenylether, Triethylamine, 4-Dimethylaminopyridine, dicyclohexyl carbodiimide (DCC), Hydrochloric acid (HCl), Sodium sulfate (Na_2SO_4), 3-[4,5-dimethylthiazol-2yl]-2,5-diphenyl tetrazolium bromide (MTT), Phosphate Buffered Saline (PBS), Roswell Park Memorial Institute (RPMI). As solvents, Milli-Q water (18.2 MΩ, filtered with filter pore size 0.22 μM) from Millipore, toluene, ethanol, acetone, dimethylsulphoxide (DMSO), hexane, chloroform, dichloromethane and tetrahydrofuran were used anhydrous and HPLC grade.

4.2. Synthesis of the Nanoparticles.

Synthesis of Iron Oleate. The synthesis was done following a published procedure.[23] A mixture of 10.8 g of iron chloride (40 mmol) and 36.5 g of sodium oleate (120 mmol) were solved in 80 ml of ethanol, 60 ml of distilled water and 140 ml of hexane. The resulting solution was heated till 60 °C and let for 4 h allowing a reflux of hexane and in inert atmosphere. At that time, the reaction was cooled down to room temperature and two phases could be distinguished: a lower aqueous phase and an upper organic phase,

containing the iron oleate. The organic phase was washed 3 times with distilled water and the hexane was evaporated in the rotavapor.

Synthesis of Iron-Manganese Oleate. Briefly, a mixture of 10.8 g of iron chloride (40 mmol), 3.96 g of manganese chloride (20 mmol) and 48.71 g of sodium oleate (160 mmol) were solved in 100 mL of ethanol, 100 mL of milli-Q water and 200 mL of hexane. Then, the protocol described above for the iron oleate synthesis was performed.

Synthesis of Fe1. 1.8 g (2 mmol) of the previously prepared iron oleate, 0.57 g (2 mmol) of oleic acid, and 1.61 g (6 mmol) oleic alcohol were weighed and solved in 10 g of Diphenyl ether. Then, under an inert atmosphere, the mixture was heated up to a temperature of 250 °C (following a heating ramp of 10 °C / min). Once this temperature was reached, it was maintained for 30 min, and then cooled to room temperature. After this procedure, it was necessary to carry out a protocol for washing and purification of the NPs: first NPs were washed several times adding acetone-ethanol (ratio 1:1) in order to precipitate them, then they were centrifuged at 5.000 rpm for 10 min, and finally the nanoparticles were suspended in toluene.

Synthesis of MnFe1. 1.8 g (2 mmol) of the previously prepared iron-manganese oleate, 0.57 g (2 mmol) of oleic acid, and 1.61 g (6 mmol) oleic alcohol were weighed and solved in 10 g of Diphenyl ether. Then, the same protocol described for Fe1 was performed. Finally the nanoparticles MnFe1 were suspended in toluene.

Synthesis of Fe2. 1.8 g (2 mmol) of the previously prepared iron oleate and 0.285 g (1 mmol) of oleic acid were solved in 15 ml of 1-octadecene. This solution was heated to 200 °C under inert atmosphere, and subsequently raised to 320 °C with a heating ramp of 1 °C / min. The synthesis was maintained at that temperature for 1 h, and then the reaction was cooled down. After this procedure, the same purification method commented above

in the synthesis of Fe1 was carried out. Finally the nanoparticles Fe2 were suspended in toluene.

Synthesis of MnFe2. 1.8 g (2 mmol) of the previously prepared iron-manganese oleate and 0.285 g (1 mmol) of oleic acid were solved in 6 mL of 1-octadecene. Then, the same protocol described for Fe2 was performed. Finally the nanoparticles MnFe2 were suspended in toluene.

4.3. Synthesis of the Ligand.

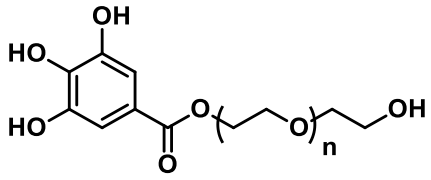

The gallol-PEGn-OH was synthesized following the previously synthetic route reported by us.[24, 35, 36] In brief, to a solution of poly ethylene glycol (Mw: 3000 g/mol, 1 mmol, 3.0 g), gallic acid (Mw: 170 g/mol, 1 mmol, 170 mg) and 4-(dimethylamino) pyridine (Mw: 122 g/mol, 200 μmol, 24 mg) in 100 mL of tetrahydrofuran and 10 mL of dichloromethane, in a round-bottom flask under nitrogen atmosphere, was added dropwise a solution of dicyclohexyl carbodiimide (Mw: 206 g/mol, 5 mmol, 1 g). The mixture was stirred overnight at room temperature. The reaction mixture was filtered through a filter paper and solvents were rota-evaporated. The crude product was dissolved in 100 mL of milli-Q water and the solution was adjusted to pH 2 by adding few mL of a 0.1 mM HCl solution. The product was extracted from the water phase with dichloromethane (100 mL, three times). The organic layer was dried over Na_2SO_4, filtered through a filter paper and the solvent was rota-evaporated. ^{1}H NMR spectroscopy confirmed the desired product gallol-PEG-OH. ^{1}H NMR (400 MHz, $CDCl_3$) δ (ppm): 7.22 (s, 2H), 4.43-4.40 (m, 2H), 3.85-3.45 (m, CH_2-PEG, -OH). FTIR peaks (cm^{-1}): 1466

(C-H bend vibration), 1359 (C-H bend vibration), 1341 (C-H bend vibration), 1307 (anti-symmetric stretch vibration), 1268 (C-O stretch vibration), 1238 (C-O stretch vibration), 1092 (C-O-C stretch vibration), 942 (CH out-of-plane bending vibration).

4.4. Functionalization of MNPs.

The functionalization of the MNPs was performed following the previously protocol published.[38] Briefly, in a separating funnel was added a solution of 1.0 mL of ferrite/manganese ferrite nanoparticles (10 g/L of Fe, Mn), 1.0 mL of the gallol-PEGn-OH derived in a concentration of 0.1 M in $CHCl_3$ and 50 µL of triethylamine. The mixture was shaked gently and it was diluted with 5 mL of toluene, 5 mL of milli-Q water and 10 mL of acetone. Then, it was shaken and the nanoparticles were transferred into the aqueous phase. After that, the aqueous phase was collected in a round-bottom flask and the residual organic solvents were rota-evaporated. Then, the gallol derived MNPs were purified in centrifuge filters with a molecular weight cut-off of 100 kDa at 450 rcf. In each centrifugation, the functionalized MNPs were re-suspended with milli-Q water. The purification step was repeated several times until the filtered solution was cleared. Then, the gallol derived MNPs were re-suspended in PBS buffer. Finally, to ensure high stable mono-dispersed magnetic nanoparticles, the solution of MNPs was centrifuged at 150 rcf for 5 min and also, it was placed onto a permanent magnet (0.6 T) for 5 min.

4.5. Characterization Methods.

Nuclear Magnetic Resonance Spectroscopy (NMR). ^{1}H-NMR spectra of samples prepared in $CDCl_3$ were recorded on a NMR Bruker Ascend 400MHz spectrometer.

Fourier Transform Infra-Red Spectroscopy (FTIR). FTIR spectra were recorded with a FTIR-4100 Jasco using a single reflection ATR accessory (MIRacle ATR, PIKE Technologies) coupled to a liquid nitrogen cooled mercury cadmium telluride (MCT) detector. All spectra were recorded in the 4000 to 800 cm^{-1} range at 4 cm^{-1} resolution and accumulating 50 scans. Gallol derived ligands were deposited as solid product and magnetic nanoparticles were prepared by dropcasting of a highly concentrated nanoparticle solution onto a microscope slide (Thermo Scientific).

Transmission Electron Microscopy. TEM images were obtained on a FEI Tecnai G2 Twin microscope operated at an accelerating voltage of 100 kV. TEM samples were prepared by dropping a solution of the corresponding magnetic nanoparticles at ~1 g/L of Fe, Mn on a carbon-coated copper grid and letting the solvent evaporate. The diameters were calculated on an average of hundred nanoparticles measured.

Dynamic Light Scattering (DLS). The size distribution and zeta potential measurements of the gallol derived magnetic nanoparticles were performed on a Zetasizer Nano ZS90 (Malvern, USA). The nanoparticles were dispersed in milli-Q water or PBS at a concentration of 50 mg/L of Fe, Mn. The measurements were done on a cell type: ZEN0118-low volume disposable sizing cuvette, setting 2.420 as refractive index with 173º Backscatter (NIBS default) as angle of detection. The measurement duration was set as automatic and three as the number of measurements. As analysis model the general purpose (normal resolution) was chosen. For the size distribution measurement, the number mean was selected.

Inductively Coupled Plasma High Resolution Mass Spectroscopy (ICP-HRMS). Fe and Mn concentrations were determined on an ICP-HRMS. The magnetic nanoparticles were digested with aqua regia (a mixture of three parts of HNO_3 and one part of HCl). Briefly,

2.5 mL of aqua regia were added to 25 μL of a solution of nanoparticles in a volumetric flask. The mixture was left overnight. Then, milli-Q water was added to complete the total volume of 25 mL.

In vitro longitudinal and transversal relaxivities (r_1 and r_2). r_1 and r_2 relaxivities were calculated at two different magnetic fields, 1.5 T (Bruker Minispec) and 9.4 T (Bruker Biospec) using concentrations of gallol derived nanoparticles between 2.3 to and 0.1 mM of Fe, Mn in physiological conditions, at 37 ºC. T_1 was determined either using inversion-recovery or saturation recovery sequences and T_2 was determined using the Carl-Purcell-Meiboom-Gill (CPMG) sequence. r_1 and r_2 relaxivities at high field (9.4 T) were measured on a Bruker Biospec MRI system equipped with 400 mT m^{-1} field gradients and a 40 mm quadrature bird-cage resonator at 298 K. T_1 values were determined using a saturation-recovery spin-echo sequence (TR values from 50 ms to 10 s) and T_2 values using a 64-echo Carl-Purcell-Meiboom-Gill (CPMG) sequence (TE values from 7.5 ms to 640 ms). Regions of interest (ROIs) were drawn on the first image of the image sequence and the intensity values extracted and fit to the following equations:

$$M_Z(t) = M_0(1 - e^{-TR/T_1})$$

$$M_{XY}(t) = M_0 e^{-TE/T_2}$$

Where M_z and M_{xy} are the signal intensities at time TR or TE, and M_0 is the signal intensity at equilibrium.

Cell Culture. Mouse microglia cell line N13 were cultured in Roswell Park Memorial Institute medium (RPMI) supplemented with 2 mM L-glutamine, 10 % fetal bovine serum (FBS) and 1 % penicillin/streptomycin at 37 ºC in an incubator with a humidified atmosphere with 5 % CO_2.

Cytotoxicity assays. Briefly, the N-13 cells were plated at a density of 1 x 10^4 cells/well in a 96-well plate at 37 ºC in 5 % CO_2 atmosphere (200 µL per well, number of repetitions = 5). After 24 h of culture, the medium in the wells was replaced with fresh medium containing gallol derived magnetic nanoparticles in varying concentrations from 0.1 µg/mL to 100 µg/mL. After 24 h, the supernatant of each well was replaced by 200 µL of fresh medium with 3-[4,5-dimethylthiazol-2-yl]-2,5-diphenyl tetrazolium bromide (MTT) (0.5 mg/mL). After 2 h of incubation at 37 ºC and 5 % CO_2 the medium was removed and the formazan crystals were solubilized with 200 µL of DMSO, and the solution was vigorously mixed to dissolve the reacted dye. Two controls were performed to evaluate the cytotoxicity: as negative control, cells unexposed to MNPs were used, and as positive control, the cells were exposed to Triton X-100 (1 % v/v) for 15 min prior to the MTT procedure. The absorbance of each well was read on a microplate reader (Dynatech MR7000 instruments) at 550 nm. The relative cell viability (%) and its error related to control wells containing cell culture medium without nanoparticles were calculated by the equations:

$$\textbf{\textit{Relative Cell Viability}}\ (\textbf{\textit{RCV}})\ (\%) = \frac{[\textbf{\textit{Abs}}]\textbf{\textit{test}} - [\textbf{\textit{Abs}}]\ \textbf{\textit{Pos.Control}}}{[\textbf{\textit{Abs}}]\ \textbf{\textit{Neg.Control}} - [\textbf{\textit{Abs}}]\ \textbf{\textit{Pos.Control}}} \times \mathbf{100}$$

$$\textbf{\textit{Error}}\ (\%) = \mathbf{RCVtest} \times \sqrt{\left(\frac{[\boldsymbol{\sigma}]\mathbf{test}}{[\mathbf{Abs}]\mathbf{test}}\right)^{\mathbf{2}} + \left(\frac{[\boldsymbol{\sigma}]\mathbf{control}}{[\mathbf{Abs}]\mathbf{control}}\right)^{\mathbf{2}}}$$

where σ is the standard deviation.

Non parametric tests were used for statistical analysis using IBM SPSS package v22.

Teratogenicity assay. Wild type zebrafish were outcrossed at day 0. Embryos well collected and incubated at 28 ºC in E3 medium for 4 h. Not fertilized eggs were then removed. Properly developing embryos were then incubated with different concentrations of the test products dissolved in E3 medium. 20-30 eggs were placed in 8-well square

petri-dishes in a volume of 4 mL. Survival, hatching and malformations were observed in 24, 48, 72 and 144 hpf when experiments were finished

In vivo Magnetic Resonance Imaging. In vivo mice experiments were performed in accordance with the ethical guidelines of Andalusian government. Male Balb/c mice (n = 3) with ca. 22 g in weight, provided by Janvier Labs were used. Animals were anesthetized with 1 % isoflurane, the tail vein was cannulated and then the animals were placed in the magnet, where respiration and body temperature were monitored throughout the entire MRI experiment. The magnetic nanoparticle was administered intravenously via tail vein at a concentration of 5 mg of Fe per kg of body weight.

All the MRI experiments were carried out on a 9.4 T Bruker Biospec system equipped with a 400 mT/m gradients and a 40 mm quadrature bird-cage resonator. High resolution T_2-weighted images were acquired using a turbo-RARE sequence with respiratory gating (TE = 16 ms, TR = 1000 ms, 4 averages, 156 μm in-plane resolution and 1 mm slice thickness). Quantitative T_2 measurements were also performed using a multi-echo spin echo sequence (TEs ranging from 7 ms to 448 ms, TR = 3500 ms, FOV = 4 cm, matrix size = 128x128, slice thickness = 1 mm). The time-courses were followed by using a turbo-RARE sequence with the same parameters indicated above, but only 1 average to improve temporal resolution (1 image every 30 seconds). The acquisition scheme was as follows: T_2-weighted, quantitative T_2, intravenous injection of the gallol derived magnetic nanoparticles, time-course for 35 min, quantitative T_2 and T_2 weighted. The first 35 min time courses were analyzed semi-quantitatively using the following expression:

$$\boldsymbol{RE} = \left| \frac{\boldsymbol{I_t - I_0}}{\boldsymbol{I_0}} \times \mathbf{100} \right|$$

where RE is the modulus of relative signal enhancement, I_t is the signal intensity at any given time after the nanoparticles injection, and I_0 is the signal intensity before the injection.

Long-term pharmacokinetics were measured by quantitative T_2 mapping at 0 h and 1 h. Pharmacokinetics were obtained by calculating the average values within different regions of interest (ROIs) placed on the following tissues: liver and kidneys, ~~spleen and muscle~~.

Statistical analysis. The statistical analysis was performed using the SPSS package (SPSS Inc., Chicago, Illinois). Cell viability, hatching, survival rates of embryos, *in vivo* T_2 values and weight variation are shown as mean ± standard deviation (SD). Student's t-test or two-way analysis of variance were used to determine significant differences between different MNPs or different experimental conditions. The level of significance was set at $p<0.05$.

Supporting Information

DLS/zeta potential, FTIR, *In vitro* relaxivities, Stability studies, Cytotoxicity assays and Teratogenicity assays.

Acknowledgements

Financial support was provided by the Andalusian Ministry of Health (PI2013-0559 to MPL), the Spanish Ministry of Economy and Competitiveness (CTQ2017-86655-R to MPL and MLGM). MPL thanks to the V Plan Propio of the University of Seville for the Postdoctoral Fellowship. The authors thank Juan F. López and M. Carmen Muñoz-Hernández for assistance with TEM and MRI experiments.

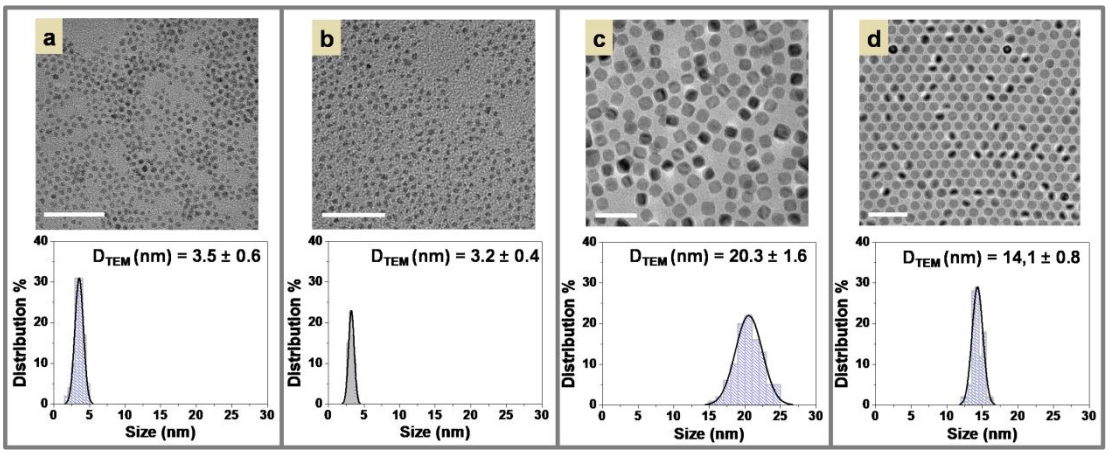

Figure 1. TEM images of the four different nanoparticles (left): Fe1 (a), MnFe1 (b), Fe2 (c) and MnFe2 (d). The scale bar is equivalent to 50 nm in all the images. The size distribution histograms are shown in each case. Diameters are expressed as the mean ± SD, by measuring at least 100 particles.

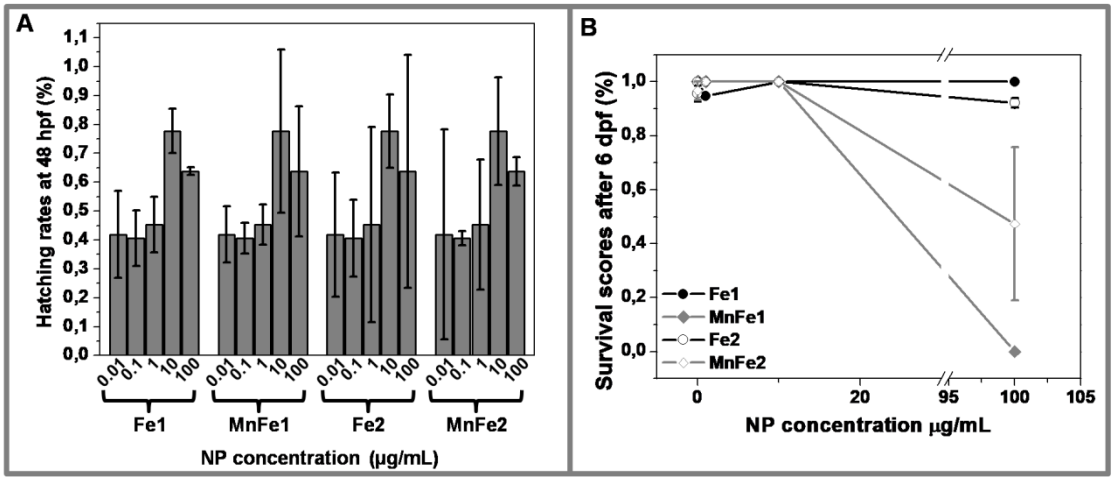

Figure 2. A) Hatching rate of zebrafish embryos exposed to MNP at different concentration 48 hpf B). Dose-dependent survival rate of the zebrafish embryos exposed to MNP at 6 dpf. All data are expressed as the mean ± SD by analyzing 20-30 eggs per NP concentration.

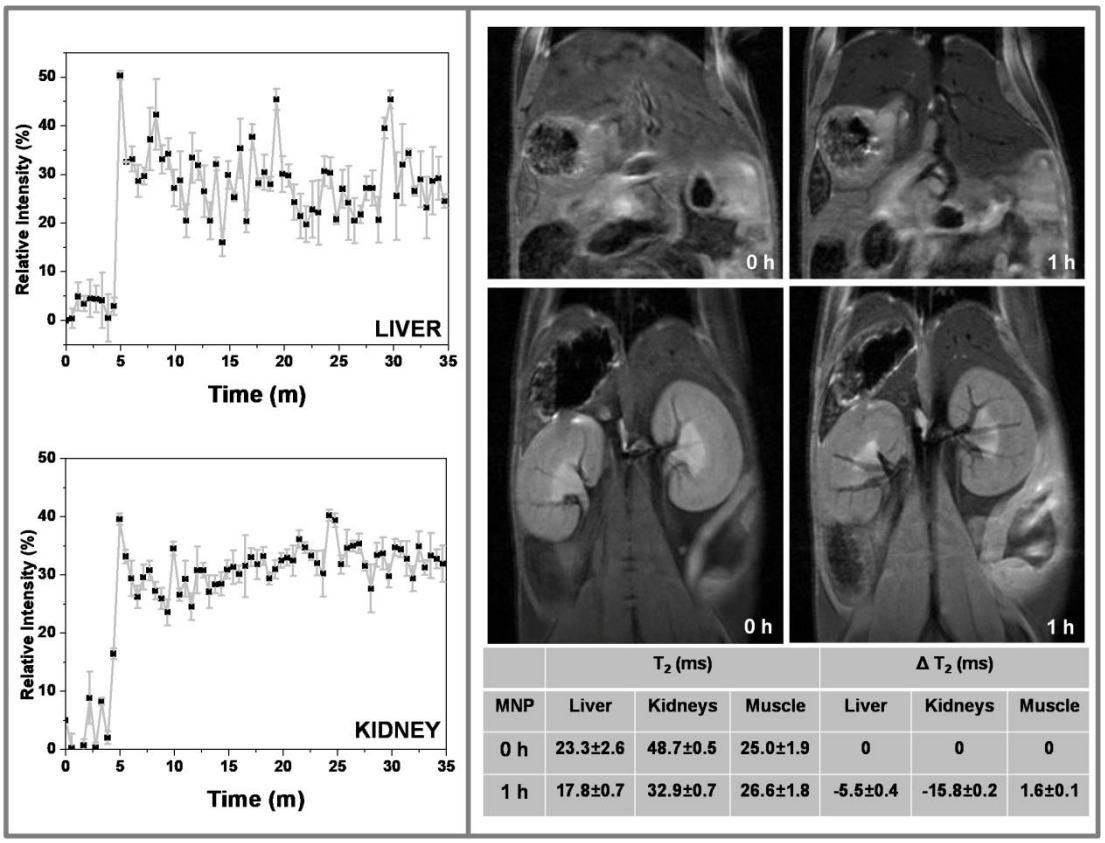

	T_2 (ms)			ΔT_2 (ms)		
MNP	Liver	Kidneys	Muscle	Liver	Kidneys	Muscle
0 h	23.3±2.6	48.7±0.5	25.0±1.9	0	0	0
1 h	17.8±0.7	32.9±0.7	26.6±1.8	-5.5±0.4	-15.8±0.2	1.6±0.1

Figure 3. Left) In vivo time courses of Fe2 after intravenously injection in balb/c mice: top) Liver; bottom) Kidneys. Right). Representative T_2-weighted MR images at different experimental times after the intravenous injection of Fe2. top) T_2-weighted images of liver at 0 and 1 h after injection. bottom) T_2-weighted images of kidneys and muscle at 0 and 1 h respectively after injection. Table: T_2 quantitative averages and ΔT_2 values of liver, kidneys and muscle at different times after intravenously injection of Fe2. The average values were obtained by performing three experiments.

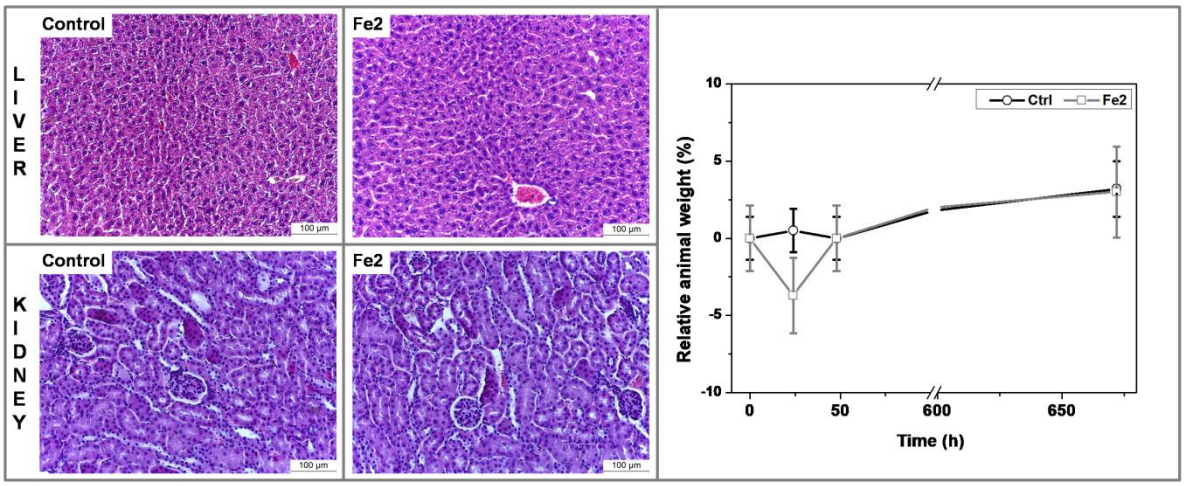

Figure 4. Representative histological sections of: liver, control (a) and Fe2 injected (b); and kidney, control (c) and Fe2 injected (d). (Right) Weight profile of intravenously injected mice and control mice in relative values. Data are expressed as the mean ± SD (n=3).

References

[1] Bogart LK, Pourroy G, Murphy CJ, Puntes V, Pellegrino T, Rosenblum D, et al. Nanoparticles for Imaging, Sensing, and Therapeutic Intervention. ACS Nano 2014;8:3107-22.

[2] Kreyling WG, Abdelmonem AM, Ali Z, Alves F, Geiser M, Haberl N, et al. In vivo integrity of polymer-coated gold nanoparticles. Nature Nanotechnology 2015;10:619.

[3] Caro C, Dalmases M, Figuerola A, García-Martín ML, Leal MP. Highly water-stable rare ternary Ag–Au–Se nanocomposites as long blood circulation time X-ray computed tomography contrast agents. Nanoscale 2017;9:7242-51.

[4] Caro C, Pozo D. Polysaccharide colloids as smart vehicles in cancer therapy. Current Pharmaceutical Design 2015;21:4822-36.

[5] Chen L, Watson C, Morsch M, Cole NJ, Chung RS, Saunders DN, et al. Improving the Delivery of SOD1 Antisense Oligonucleotides to Motor Neurons Using Calcium Phosphate-Lipid Nanoparticles. Frontiers in Neuroscience 2017;11.

[6] Becerro AI, Fuente JMdl, García-Martín ML, González-Mancebo D, Ocaña M, Rojas TC. HoF3 and DyF3 Nanoparticles as Contrast Agents for High-Field Magnetic Resonance Imaging. 2017.

[7] Lahooti A, Sarkar S, Laurent S, Shanehsazzadeh S. Dual nano-sized contrast agents in PET/MRI: a systematic review. Contrast Media & Molecular Imaging 2016;11:428-47.

[8] Materia ME, Pernia Leal M, Scotto M, Balakrishnan PB, Kumar Avugadda S, García-Martín ML, et al. Multifunctional Magnetic and Upconverting Nanobeads as Dual Modal Imaging Tools. Bioconjugate Chemistry 2017;28:2707-14.

[9] Toth GB, Varallyay CG, Horvath A, Bashir MR, Choyke PL, Daldrup-Link HE, et al. Current and potential imaging applications of ferumoxytol for magnetic resonance imaging. Kidney Int 2017;92:47-66.

[10] Ventola CL. Progress in Nanomedicine: Approved and Investigational Nanodrugs. P T 2017;42:742-55.

[11] Eskandari N, Nejadi Babadaei MM, Nikpur S, Ghasrahmad G, Attar F, Heshmati M, et al. Biophysical, docking, and cellular studies on the effects of cerium oxide nanoparticles on blood components: in vitro. International journal of nanomedicine 2018;13:4575-89.

[12] Liegertová M, Wrobel D, Herma R, Müllerová M, Šťastná LČ, Cuřínová P, et al. Evaluation of toxicological and teratogenic effects of carbosilane glucose glycodendrimers in zebrafish embryos and model rodent cell lines. Nanotoxicology 2018.

[13] Huang H, Delikanli S, Zeng H, Ferkey DM, Pralle A. Remote control of ion channels and neurons through magnetic-field heating of nanoparticles. Nature Nanotechnology 2010;5:602.

[14] Doubrovinski K, Swan M, Polyakov O, Wieschaus EF. Measurement of cortical elasticity in Drosophila melanogaster embryos using ferrofluids. Proceedings of the National Academy of Sciences 2017;114:1051.

[15] Schilling TF, Webb J. Considering the zebrafish in a comparative context. Journal of Experimental Zoology Part B: Molecular and Developmental Evolution 2007;308B:515-22.

[16] Fleming A, Alderton WK. Zebrafish in pharmaceutical industry research: Finding the best fit. Drug Discovery Today: Disease Models 2013;10:e43-e50.

[17] George S, Xia T, Rallo R, Zhao Y, Ji Z, Lin S, et al. Use of a high-throughput screening approach coupled with in vivo zebrafish embryo screening to develop hazard ranking for engineered nanomaterials. ACS Nano 2011;5:1805-17.

[18] Rizzo LY, Golombek SK, Mertens ME, Pan Y, Laaf D, Broda J, et al. In vivo nanotoxicity testing using the zebrafish embryo assay. Journal of Materials Chemistry B 2013;1:3918-25.

[19] Zhu X, Tian S, Cai Z. Toxicity Assessment of Iron Oxide Nanoparticles in Zebrafish (Danio rerio) Early Life Stages. PLOS ONE 2012;7:e46286.

[20] Felix LC, Ortega VA, Ede JD, Goss GG. Physicochemical Characteristics of Polymer-Coated Metal-Oxide Nanoparticles and their Toxicological Effects on Zebrafish (Danio rerio) Development. Environmental Science & Technology 2013;47:6589-96.

[21] Zhang Y, Zhu L, Zhou Y, Chen J. Accumulation and elimination of iron oxide nanomaterials in zebrafish (Danio rerio) upon chronic aqueous exposure. Journal of Environmental Sciences 2015;30:223-30.

[22] Lee J-H, Huh Y-M, Jun Y-w, Seo J-w, Jang J-t, Song H-T, et al. Artificially engineered magnetic nanoparticles for ultra-sensitive molecular imaging. Nature Medicine 2006;13:95.

[23] Park J, An K, Hwang Y, Park JEG, Noh HJ, Kim JY, et al. Ultra-large-scale syntheses of monodisperse nanocrystals. Nature materials 2004;3:891-5.

[24] Pernia Leal M, Rivera-Fernández S, Franco JM, Pozo D, De La Fuente JM, García-Martín ML. Long-circulating PEGylated manganese ferrite nanoparticles for MRI-based molecular imaging. Nanoscale 2015;7:2050-9.

[25] Materia ME, Guardia P, Sathya A, Pernia Leal M, Marotta R, Di Corato R, et al. Mesoscale assemblies of iron oxide nanocubes as heat mediators and image contrast agents. Langmuir 2015;31:808-16.

[26] Kakwere H, Leal MP, Materia ME, Curcio A, Guardia P, Niculaes D, et al. Functionalization of Strongly Interacting Magnetic Nanocubes with (Thermo)Responsive Coating and Their Application in Hyperthermia and Heat-Triggered Drug Delivery. ACS Applied Materials & Interfaces 2015;7:10132-45.

[27] Yang L, Ma L, Xin J, Li A, Sun C, Wei R, et al. Composition Tunable Manganese Ferrite Nanoparticles for Optimized T2 Contrast Ability. Chemistry of Materials 2017;29:3038-47.

[28] Guo Y, Chen L, Wu J, Hua J, Yang L, Wang Q, et al. Parental co-exposure to bisphenol A and nano-TiO2 causes thyroid endocrine disruption and developmental neurotoxicity in zebrafish offspring. Science of The Total Environment 2019;650:557-65.

[29] Pham DH, De Roo B, Nguyen XB, Vervaele M, Kecskés A, Ny A, et al. Use of Zebrafish Larvae as a Multi-Endpoint Platform to Characterize the Toxicity Profile of Silica Nanoparticles. Scientific Reports 2016;6.

[30] Cáceres-Vélez PR, Fascineli ML, Grisolia CK, de Oliveira Lima EC, Sousa MH, de Morais PC, et al. Genotoxic and histopathological biomarkers for assessing the effects of magnetic exfoliated vermiculite and exfoliated vermiculite in Danio rerio. Sci Total Environ 2016;551-552:228-37.

[31] Dobson AW, Erikson KM, Aschner M. Manganese Neurotoxicity. Annals of the New York Academy of Sciences 2004;1012:115-28.

[32] Caro C, García-Martín ML, Pernia Leal M. Manganese-Based Nanogels as pH Switches for Magnetic Resonance Imaging. Biomacromolecules 2017;18:1617-23.

[33] Ahmad F, Liu X, Zhou Y, Yao H. An in vivo evaluation of acute toxicity of cobalt ferrite (CoFe2O4) nanoparticles in larval-embryo Zebrafish (Danio rerio). Aquatic Toxicology 2015;166:21-8.

[34] Caro C, Carmen Muñoz-Hernández M, Leal MP, García-Martín ML. In vivo pharmacokinetics of magnetic nanoparticles. Methods in Molecular Biology2018. p. 409-19.

[35] Leal MP, Muñoz-Hernández C, Berry CC, García-Martín ML. In vivo pharmacokinetics of T2 contrast agents based on iron oxide nanoparticles: optimization of blood circulation times. RSC Advances 2015;5:76883-91.

[36] Pernia Leal M, Caro C, García-Martín ML. Shedding light on zwitterionic magnetic nanoparticles: Limitations for in vivo applications. Nanoscale 2017;9:8176-84.

[37] Peter AI, Naidu ECS, Akang E, Ogedengbe OO, Offor U, Rambharose S, et al. Investigating Organ Toxicity Profile of Tenofovir and Tenofovir Nanoparticle on the Liver and Kidney: Experimental Animal Study. Toxicological Research 2018;34:221-9.

[38] Riedinger A, Pernia Leal M, Deka SR, George C, Franchini IR, Falqui A, et al. "nanohybrids" based on pH-responsive hydrogels and inorganic nanoparticles for drug delivery and sensor applications. Nano Letters 2011;11:3136-41.

1